Decade-long time-monitoring of candidate luminous blue variable stars in the two very metal-deficient star-forming galaxies DDO 68 and PHL 293B

N. G. Guseva, T. X. Thuan, Y. I. Izotov

Monthly Notices of the ROYAL ASTRONOMICAL SOCIETY

MNRAS **512,** 4298–4307 (2022) https://doi.org/10.1093/mnras/stac820
Advance Access publication 2022 March 25

Decade-long time-monitoring of candidate luminous blue variable stars in the two very metal-deficient star-forming galaxies DDO 68 and PHL 293B

N. G. Guseva,[1]★ T. X. Thuan[2,3]★ and Y. I. Izotov[1]★

[1]*Bogolyubov Institute for Theoretical Physics, Ukrainian National Academy of Sciences, Metrologichna 14b, UA-03143 Kyiv, Ukraine*
[2]*Astronomy Department, University of Virginia, P.O. Box 400325, Charlottesville, VA 22904-4325, USA*
[3]*Institut d'Astrophysique de Paris (UMR 7095 CNRS & Sorbonne Université) 98 bis Bd Arago, F-75014 Paris, France*

Accepted 2022 March 21. Received 2022 March 20; in original form 2022 February 18

ABSTRACT

We have studied the spectral time variations of candidate luminous blue variable (cLBV) stars in two low-metallicity star-forming galaxies, DDO 68 and PHL 293B. The LBV in DDO 68, located in H II region #3, shows an outburst, with an increase of more than 1000 times in H α luminosity during the period 2008–2010. The broad emission of the H I and He I lines display a P Cygni profile, with a relatively constant terminal velocity of $\sim$800 km s^{-1}, reaching a maximum luminosity L(H α) of $\sim 2 \times 10^{38}$ erg s^{-1}, with a full width at half-maximum (FWHM) of $\sim$1000–1200 km s^{-1}. On the other hand, since the discovery of a cLBV in 2001 in PHL 293B, the fluxes of the broad components and the broad-to-narrow flux ratios of the H I and He I emission lines in this galaxy have remained nearly constant over 16 yr, with small variations. The luminosity of the broad H α component varies between $\sim 2 \times 10^{38}$ erg s^{-1} and $\sim 10^{39}$ erg s^{-1}, with the FWHM varying in the range $\sim$500–1500 km s^{-1}. Unusually persistent P Cygni features are clearly visible until the end of 2020 despite a decrease of the broad-to-narrow flux ratio in the most recent years. A terminal velocity of $\sim$800 km s^{-1} is measured from the P Cygni profile, similar to the one in DDO 68, although the latter is 3.7 more metal-deficient than PHL 293B. The relative constancy of the broad H α luminosity in PHL 293B suggests that it is due to a long-lived stellar transient of type LBV/SN IIn.

Key words: galaxies: abundances – galaxies: dwarf – galaxies: ISM – galaxies: starburst.

1 INTRODUCTION

During their evolution, massive stars are known to go through a very short and high luminosity important transitional phase, called the luminous blue variable (LBV) phase. During this phase, LBVs undergo significant variations in photometric magnitudes and spectral features, characterized in particular by the appearance of broad components in the hydrogen and helium emission lines and in some heavy element ion lines in the ultraviolet (UV) and optical ranges. The broad emission in the LBVs may be due to sharp eruptions of the massive stars, reaching a total mass loss of up to $\sim$30–100 M$_\odot$. It can also be caused by stellar winds and expanding dense circumstellar envelopes. In these cases, H α luminosities are in the range of 10^{36}–10^{39} erg s^{-1} (Izotov, Thuan & Guseva 2007). The mass-loss rate of hydrogen-rich layers through stellar winds is $\sim 10^{-6}$–$\sim 10^{-3}$ M$_\odot$ yr^{-1} (Humphreys & Davidson 1994; Smith, Crowther & Prinja 1994; Drissen, Roy & Robert 1997; Drissen et al. 2001). However, very strong broad emission (full width at half-maximum, FWHM $>$ 1000 km s^{-1}) can also be present in the spectra of objects other than massive stars, such as Type IIn Supernovae (SNe) and active galactic nuclei (AGNs). In these objects, the luminosities of the broad H α component are larger and can reach values up to 10^{40}–10^{42} erg s^{-1} (Izotov et al. 2007; Sobral, Matthee & Darvish 2020; Burke et al. 2021; Kokubo 2021).

LBVs frequently show recurring eruptive events through various evolution phases, during their transition from young massive main-sequence stars to WR stars, SN explosions, or massive black holes. It is believed that stars with masses greater than 20–30 M$_\odot$ and luminosities $L \sim 10^3$–10^6 L$_\odot$ go through the LBV phase (Crowther 2007; Solovyeva, Vinokurov & Sarkisyan 2020). Among all types of variable stars, only LBV stars show significant variability both in photometric brightness and spectroscopic features: rapidly amplified broad emission and blueward absorption lines, strongly enhanced continuum that becomes bluer in the UV and optical spectra.

To date, about a few hundreds LBVs and candidate LBVs (cLBVs) are known to show irregular cyclic quasi-periodic brightness variations of $\sim$0.5–2 mag on time-scales from several years to decades. They are called S Dor LBVs (see e.g. Massey, Waterhouse & DeGioia-Eastwood 2000; Humphreys et al. 2013, 2017; Humphreys 2019; Grassitelli et al. 2020; Weis & Bomans 2020). On the other hand, there exists a tiny number of LBV stars that show giant eruptions, with amplitudes more than 2.5–3 mag, on time-scales of up to thousands years (Davidson & Humphreys 1997; Smith et al. 2011; Vink 2012; Weis & Bomans 2020). Well-known prototypes of this category are η Carinae and P Cygni with luminosities $\sim 10^{40}$ erg s^{-1} (Lamers, de Groot & Cassatella 1983; Davidson 1999). In some cases, the peak luminosity during the outbursts can reach $\sim 10^{42}$ erg s^{-1} (Kokubo 2021). Nearly all these known luminous LBVs are either in our Galaxy or in nearby galaxies.

High-intensity broad and very broad components of emission lines, with P Cygni profiles, have also been observed in the integral spectra

★ E-mail: nguseva@bitp.kiev.ua (NG); yizotov@bitp.kiev.ua (YI); txt@virginia.edu (TT)

of star-forming galaxies (SFGs) underlying their strong narrow emission lines produced in H II regions (see e.g. Schaerer, Contini & Pindao 1999; Guseva, Izotov & Thuan 2000; Leitherer et al. 2001; Izotov & Thuan 2008; Guseva et al. 2012). The most prominent spectral features in SFGs with LBVs are broad components of hydrogen and often helium lines with blueward absorption, and Fe II emission.

To understand the physical mechanism responsible for the broad emission, time-monitoring of the broad spectral features is necessary. The reason is that, as said previously, broad emission occurs not only in LBV spectra but also in those of SNe and AGNs. It is difficult to distinguish between these different possibilities without a long-term time monitoring of the broad features. It has now been established that a significant number of the objects detected in supernova surveys are not true supernovae, but belong to a category of objects called 'supernova impostors'. Ordinary LBVs of the S Dor type or LBVs with giant eruptions, like η Car at maximum luminosity, appear among these 'impostors'. Despite the fact that many stars with LBV features have been discovered (Weis & Bomans 2020), only a few dozen of them are confirmed as genuine Galactic and extragalactic LBVs (Wofford et al. 2020). The remaining are cLBV that require time-monitoring to confirm their true nature. A genuine LBV would show a significant enhancement of the spectral and photometric features on a time-scale of tens of years, followed by the disappearance of these features. This disappearance is necessary to rule out SNe, AGNs, or other physical mechanisms (Kokubo 2021).

In addition, it is of particular interest to understand how LBV evolution in SFGs depends on the properties of the host galaxy, such as gas metallicity, interstellar medium density, star formation rate (SFR), and specific SFR (sSFR). Only very few LBVs are known up to date in metal-poor SFGs with strong star-forming activity (see e.g. Weis & Bomans 2020, and references therein). We discuss in this paper the time monitoring over two decades of the photometric and spectroscopic properties of cLBV stars in two extremely metal-deficient dwarf SFGs, DDO 68 (located in H II region #3) with 12 + log (O/H) = 7.15 and PHL 293B with 12 + log (O/H) = 7.72. These two SFGs are the lowest metallicity galaxies where LBV stars have been detected, allowing the study of the LBV phenomenon in the extremely low metallicity regime, and shedding light of the evolution of the first generation of massive stars possibly born from primordial gas.

The paper is structured as follows: the Large Binocular Telescope (LBT)/Multi-Object Double Spectrographs (MODS) and 3.5m Apache Point Observatory (APO) observations and data reduction are described in Section 2. In Section 3, we present the study of multi-epoch optical spectra of DDO 68 #3 and PHL 293B. Finally, in Section 4, we summarize our main results.

2 OBSERVATIONS AND DATA REDUCTION

Over the course of more than a decade, starting in 2008 October, we have obtained a series of spectroscopic observations for the two SFGs DDO 68 (its H II region #3) and PHL 293B, using two different telescopes and instrumental set-ups

2.1 APO observations

The first instrumental set-up consisted of the Dual Imaging Spectrograph (DIS) mounted on the ARC 3.5m APO telescope. The blue and red channels of the DIS permitted to simultaneously observe the objects over a wide range of wavelengths. A long slit giving medium resolution (R = 5000) was used during all APO observations. The B1200 grating giving medium resolution (R = 5000) with a central wavelength of ∼4800 Å and a linear dispersion of 0.62 Å pixel^{-1} was used in the blue range. In the red range, we employ the R1200 grating with a central wavelength of ∼6600 Å and a linear dispersion of 0.56 Å pixel^{-1}. In this way, APO medium resolution spectra of the two SFGs DDO 68 #3 and PHL 293B were obtained, that span two wavelength ranges, from ∼4150 to 5400 Å in the blue range, and from ∼6000 to 7200 Å in the red range.

The journal of the APO observations, giving the observation dates, the exposure times, the slit widths, and the airmasses, are shown in Table 1.

Table 1. Journal of observations.

Date	Exposure (s)	Slit width (arcsec)	Airmass
DDO 68 #3, 3.5m APO			
2008-10-27	2700	1.5	1.24
2008-11-06	2400	1.5	1.17
2009-02-22	1800	2.0	1.53
2009-11-19	1800	2.0	1.18
2010-02-06	2700	1.5	1.36
2010-03-20	1800	1.5	1.16
2010-10.31	1500	1.5	1.13
2012-02-15	2700	1.5	1.20
2012-05-16	1800	1.5	1.27
2013-06-01	986	1.5	1.42
2016-04-09	1800	0.9	1.51
2018-04-07	1860	1.5	1.06
PHL 293B, 3.5m APO			
2010-10-06	1800	1.5	1.56
2014-11.17	2700	0.9	1.19
2015-11-06	1800	0.9	1.21
2017-12-15	1800	0.9	1.27
PHL 293B, 2 × 8.4m LBT/MODS			
2020-11-18	2700	1.2	1.19

2.2 LBT observations

For PHL 293B, one high signal-to-noise ratio spectroscopic observation was also carried out with the 2 × 8.4m LBT. We employ the LBT in the binocular mode utilizing both the MODS1 and MODS2 spectrographs, equipped with 8022 × 3088 pixel CCDs. Two gratings, one in the blue range, G400L, with a dispersion of 0.5 Å pixel^{-1}, and another in the red range, G670L, with a dispersion of 0.8 Å pixel^{-1}, were used. The PHL 293B spectrum was obtained in the wavelength range ∼3150–9500 Å with a 60 × 1.2 arcsec slit, giving a resolving power R ∼ 2000. The seeing during the observation was in the range 0.5–0.6 arcsec. Three subexposures were derived, resulting in an effective exposure time of 2 × 2700 s when adding the fluxes obtained with both spectrographs, MODS1 and MODS2. The spectrum of the spectrophotometric standard star GD 71, obtained during the LBT observation with a 5 arcsec wide slit, was used for flux calibration. It was also used to correct the red part of the PHL 293B spectrum for telluric absorption lines. The journal of the LBT observation is also shown in Table 1.

2.3 Data reduction

The 2D APO spectra were bias- and flat-field corrected, fixed for distortion and tilt of frame and background subtracted using IRAF routines. For the LBT observation, the MODS Basic CCD

Table 2. Parameters of H α narrow and broad components in DDO 68 #3 spectra, observed with the 3.5m APO telescope and presented in Fig. 1.

Date	$F^a_{\rm nar}$	FWHM$^b_{\rm nar}$	FWHM^c ([O III]4959)	$F^a_{\rm br}$	FWHM$^b_{\rm br}$	$v^{\,d}_{\rm term}$	$L^e_{\rm br}$
2008-10-27	64.26	115(2.51)	2.42	84.01	1072	706	16.2
2008-11-06	59.32	79(1.74)	2.00	66.86	1029	722	12.9
2009-02-22	47.13	88(1.92)	2.33	74.41	1006	764	14.4
2009-11-19	56.61	87(1.91)	2.16	93.66	1110	808	18.1
2010-02-06	27.58	78(1.72)	1.94	30.94	1251	749	6.0
2010-03-20	34.85	78(1.72)	2.15	49.48	1107	819	9.6
2010-10-31	56.30	78(1.71)	2.55	73.84	1130	871	14.3
2012-02-15	48.22	69(1.52)	1.86	29.10	742	...	5.6
2012-05-16	73.16	78(1.72)	1.80	31.87	734	...	6.2
2013-06-01	45.34	74(1.61)	1.61	35.82	560	...	6.9
2016-04-09	13.43	63(1.39)	1.54	2.44	326	...	0.5
2018-04-07	8.48	86(1.87)	1.63	...	...	...	0.0

[a]Fluxes of H α narrow ($F_{\rm nar}$) and broad ($F_{\rm br}$) components in units of 10^{-16} erg s^{-1} cm^{-2}.
[b]FWHM of H α narrow and broad components in units of km s^{-1}, and in angstroms (in brackets).
[c]FWHM of [O III]λ4959 Å emission line in units of angstroms.
[d]Terminal velocity in units of km s^{-1}.
[e]Luminosity of H α broad component in units of 10^{37} erg s^{-1}, calculated with a distance $D = 12.71$ Mpc, which is a mean from determinations by Cannon et al. (2014), Sacchi, Annibali & Cignoni (2016), and Makarov et al. (2017).

Table 3. Parameters of H α narrow and broad components in PHL 293B spectra, presented in Fig. 3.

Date	tel.[a]	F^b *nar*	FWHM^c *nar*	FWHM^d 4959	F^b *br*	FWHM^c *br*	F^b *v.br*	FWHM^c *v.br*	F^e *sum br*	$v^{\,f}_{\rm term}$ *br*	L^g *sum br*
2001-08-22	SDSS	238.02	235(5.1)	3.8	63.74	1379	7.86	2602	71.60	938	44.2
2010-10-06	APO	261.50	71(1.6)	2.2	27.13	181	42.99	999	70.12	702	43.2
2014-11-17	APO	71.04	66(1.4)	1.6	11.77	162	12.62	627	24.39	...	15.0
2015-11-06	APO	471.20	74(1.6)	1.6	45.96	180	95.08	705	141.04	...	87.0
2017-12-15	APO	91.16	69(1.5)	1.6	9.64	165	15.02	903	24.66	...	15.2
2020-11-18	LBT	401.30	280(6.1)	4.0	23.08	504	11.64	1320	34.72	...	21.4

[a]Telescopes: 2.5m APO (labelled as SDSS), 3.5m APO (labelled as APO), 2 × 8.4m LBT (labelled as LBT).
[b]Flux of narrow ($F_{\rm nar}$), broad ($F_{\rm br}$), and very broad ($F_{\rm v.br}$) components of H α in units of 10^{-16} erg s^{-1} cm^{-2}.
[c]FWHM of narrow, broad, and very broad components of H α in km s^{-1} and in angstroms (in brackets).
[d]FWHM of the [O III]λ4959 Å emission line in angstroms.
[e]Flux of the whole broad bump (i.e. sum of the broad and very broad components) in units of 10^{-16} erg s^{-1} cm^{-2}.
[f]Terminal velocity in units of km s^{-1}.
[g]Luminosity of the whole broad bump (i.e. the sum of broad and very broad components) in 10^{37} erg s^{-1}, calculated with the distance $D = 22.7$ Mpc of PHL 293B, the same as that adopted by Izotov & Thuan (2009).

Reduction package MODSCCDRED (Pogge 2019) was used for flat-field correction and bias subtraction. Wavelength calibrations of both LBT and APO observations were performed using spectra of comparison lamps obtained every night before and after the observations. Each 2D spectrum was aligned along the brightest part of the galaxy. After wavelength and flux calibration and removal of cosmic particle trails, all subexposures were summed. 1D spectra were then extracted along the spatial axis so that the entire bright part of the H II region falls into the selected aperture.

In summary, we have obtained 12 new APO observations of DDO 68 #3 and four new APO observations of PHL 293B, together with one new LBT spectrum of PHL 293B. To increase the time baseline for PHL 293B, we have also included in our analysis the Sloan Digital Sky Survey (SDSS) spectrum obtained with the 2.5m APO telescope on 2001 August 22 and available in the SDSS archive. This brings the total number of PHL 293B spectra to be analysed to six. More details are given in Tables 2 and 3. The spectra are shown in Figs 1, 2 and 3. The spectra are displayed in the wavelength range around H α to better emphasize the temporal changes of this line. In Fig. 2, we have also shown two spectra of PHL 293B over the whole wavelength range of observations, and that are most separated in time.

3 RESULTS

3.1 Profile decomposition

The most remarkable features in the DDO 68 #3 and PHL 293B spectra are the strong broad components with P Cygni profiles underlying the narrow nebular emission of the hydrogen and helium lines. For derive quantitative measurements of these features, we have decomposed the profiles of the hydrogen emission lines into the sum of several Gaussian profiles: a high-intensity narrow component,

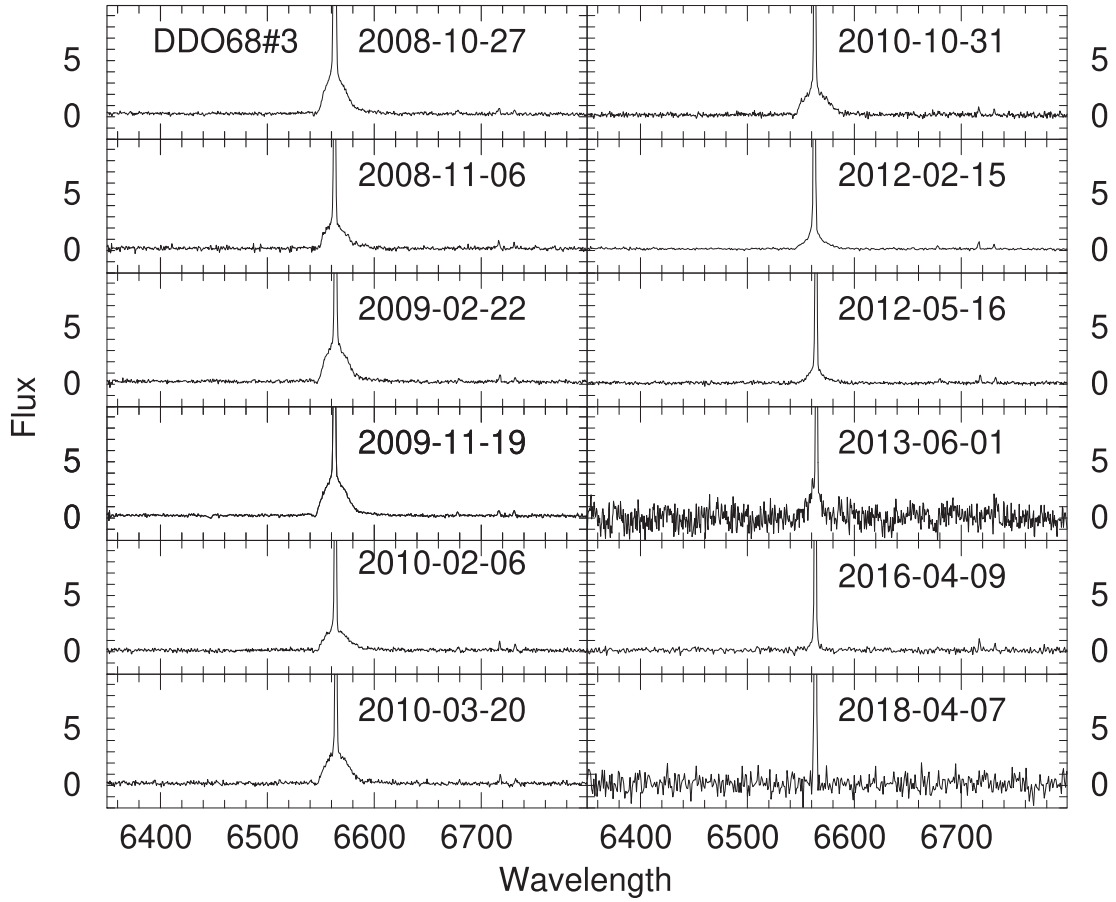

Figure 1. The rest-frame H α emission line profile in the DDO 68 #3 spectrum at different epochs, observed with the 3.5m APO telescope. Wavelengths are in Å and fluxes are in units of 10^{-16} erg s^{-1} cm^{-2} Å^{-1}.

and low-intensity broad and very broad (the latter when needed) components, using the IRAF/SPLOT deblending routine.

The fluxes and FWHM of the H α narrow and broad components, along with the terminal velocities and the total luminosities of the broad components in the two SFGs are given in Tables 2 and 3 for all spectra shown in Figs 1 and 3. The data for the very broad components in PHL 293B are also given in Table 3. Details of the profile decomposition of the H α line can be seen in Figs 4, 5, and 6. For luminosity determination, the observed fluxes of narrow and broad emission lines were corrected for the extinction and underlying stellar absorption taken from Izotov & Thuan (2009), derived in accordance with the prescription of Izotov, Thuan & Lipovetsky (1994). Note that the extinction coefficient C(H β) and equivalent width of the underlying absorption (EW$_{abs}$) derived from the high signal-to-noise ratio MMT spectrum of DDO 68 #3 and the VLT spectrum of PHL 293B (see table 3 in Izotov & Thuan 2009) are very small in both galaxies. C(H β) and EW$_{abs}$ have zero values in DDO 68 #3 and are, respectively, equal to 0.08 and 0.05 in PHL 293B.

3.2 DDO 68 #3

DDO 68 (UGC 05340) is one of the most metal-deficient SFG known (12 + logO/H = 7.15 ± 0.04, 7.14 ± 0.07; Izotov & Thuan 2009; Annibali et al. 2019a). It is likely in the process of forming by hierarchical merging (Pustilnik et al. 2017; Annibali et al. 2019b). Broad spectral features with blueshifted absorption in the lines of the hydrogen series as well as in some He I lines were first noticed in DDO 68 by Pustilnik et al. (2008). Those authors attributed the broad features to the outburst of an LBV located in one of the H II region of DDO 68 named Knot 3, and which we will designate by #3 in the remainder of this paper.

Based on photometric and spectroscopic observations, Izotov & Thuan (2009) dated the start of the strong LBV outburst in DDO 68 #3 to be between 2007 February and 2008 January. They confirmed the presence of P Cygni profiles in both the H I and He I emission lines and found that the Fe II emission lines are not present, in contrast to 'typical' LBVs (Pustilnik et al. 2008; Izotov & Thuan 2009). The absence of Fe II could be due to extremely low metallicity and thus low optical depth precluding considerable radiative pumping. Pustilnik et al. (2017) described the state of the LBV in 2015–2016 as being in a fading phase. Observations carried out by Annibali et al. (2019a) with LBT/MODS1 and LBT/MODS2 in 2017 February do not show the characteristic signs of an LBV star. This led them to conclude that, by 2017, the LBV was back in a quiescent phase.

We provide here a more complete picture of the time evolution of the LBV in DDO 68 #3 by monitoring its spectrum. Our observations start from 2008, and occur as often and as regularly as possible afterwards, ending in 2018. We show in Fig. 1 the time evolution of the H α line. We emphasize that all spectra were obtained with the same telescope and instrumental setup (3.5m APO/DIS) and reduced in a uniform manner, so they are directly comparable. We remark that, as seen in Fig. 1 and more clearly in Fig. 4, the [N II] emission lines near H α are nearly not detected, due to the low metallicity of DDO 68 #3.

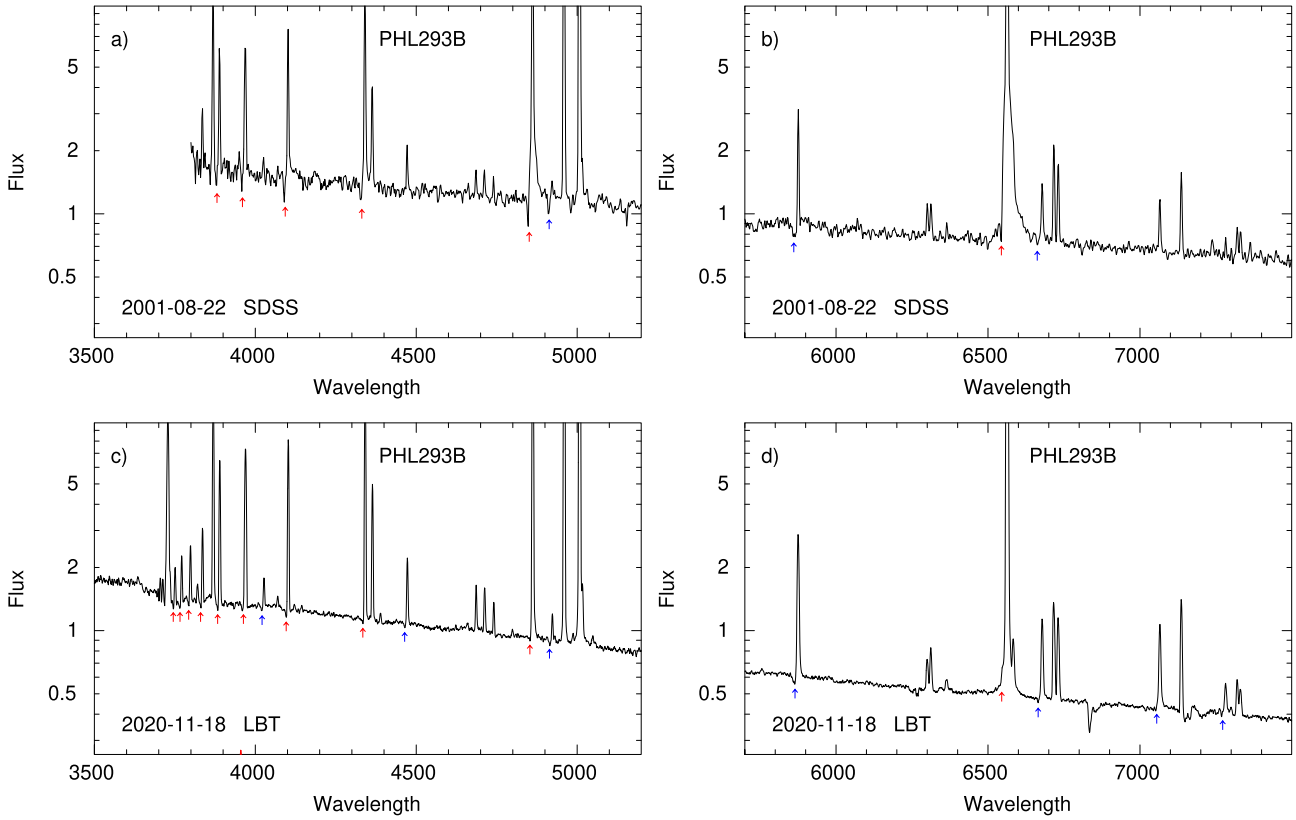

Figure 2. The most time-separated spectra of PHL 293B. Panels (a) and (b) show blue and red parts of the SDSS spectrum obtained with the 2.5m APO telescope on 2001 August 22. Panels (c) and (d) show the spectrum obtained with LBT/MODS on 2018 November 18. Absorption features of P Cygni profiles for hydrogen and helium emission lines are indicated in the rest-frame spectra by red and blue arrows, respectively. Wavelengths are in Å and fluxes are in units of 10^{-16} erg s^{-1} cm^{-2} Å^{-1}.

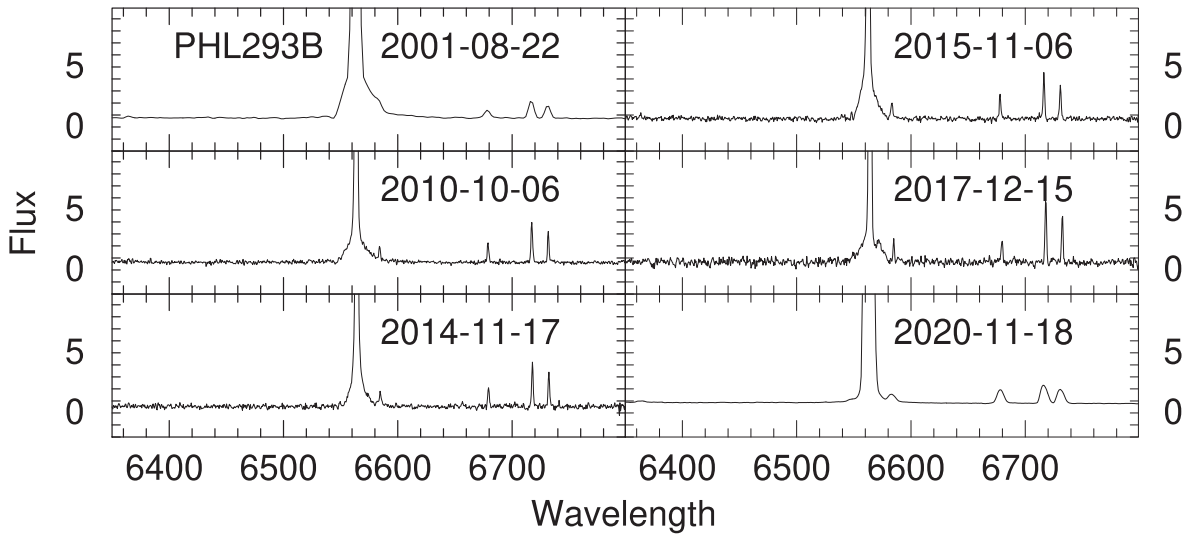

Figure 3. The rest-frame H α emission line profiles in the PHL 293B spectra at the different epochs listed in Table 3. Wavelengths are in Å and fluxes are in units of 10^{-16} erg s^{-1} cm^{-2} Å^{-1}.

Our new APO observations in the monitoring series of DDO 68 #3 reveal that the fluxes of the H α broad components are nearly an order of magnitude higher at the end of 2008 October as compared to 2008 January, when the LBV was discovered by Pustilnik et al. (2008) (Table 2 and Fig. 7b, thick solid black line). The MMT observation of DDO 68 #3 on 2008 March of Izotov & Thuan (2009) is consistent with that trend. It showed a broad H β flux $\sim$2 times lower than the one in the first observation in our APO monitoring series starting 6 months later, in 2008 October.

Our more than a decade APO monitoring showed that the features characteristic of eruption in the LBV in DDO 68 #3 persist until the period somewhere between the end of 2010 and the beginning of

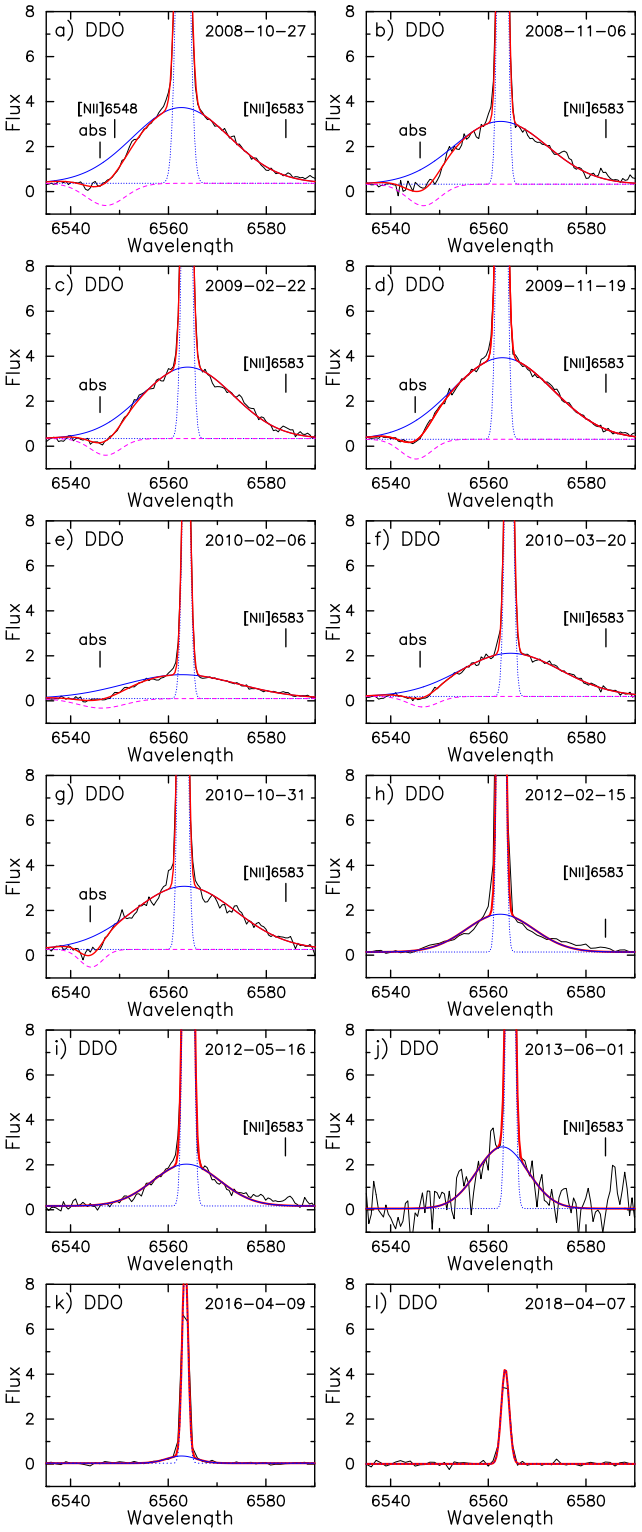

Figure 4. Decomposition by Gaussians of the H α narrow (blue dotted lines) and broad emission (blue solid lines) profiles in the spectra of DDO 68 #3, listed in Table 2 and shown in Fig. 1. The observed profile is shown by the black solid line whereas the summed flux of narrow + broad components is represented by the red solid line. Wavelengths are in Å and fluxes are in units of 10^{-16} erg s^{-1} cm^{-2} Å^{-1}.

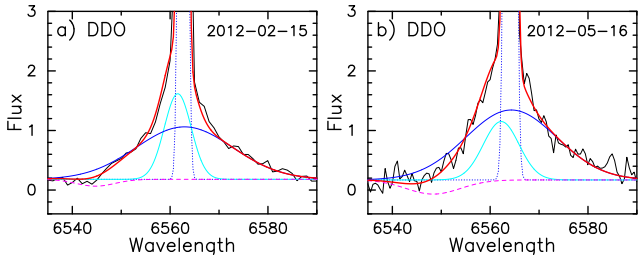

Figure 5. The observed profile of H α in DDO 68 #3 with an excess flux at high velocities in redward wings. This excess is seen only for the observations on 2012 February 15 and May 16 (see Figs 4h and i). Three Gaussians were used to fit the narrow, broad, and very broad components (blue dots, turquoise solid, and blue solid lines, respectively). The total fitted profile is represented by a red solid line. Wavelengths are in Å and fluxes are in units of 10^{-16} erg s^{-1} cm^{-2} Å^{-1}.

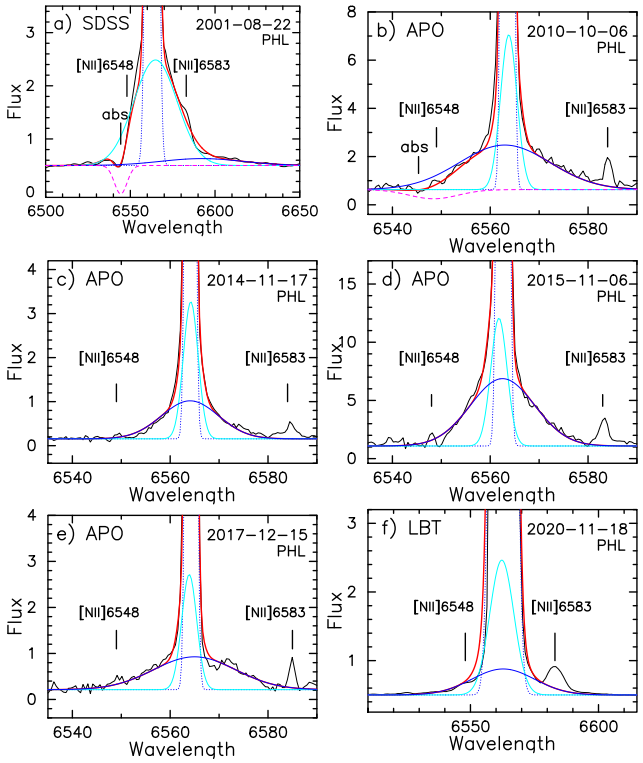

Figure 6. The H α profiles in the PHL 293B spectra obtained with different telescopes during different epochs. The black lines represent the observed spectra. The fits of H α by three or four Gaussians are shown by blue dotted lines (narrow component), by turquoise solid lines (broad component), by blue solid lines (very broad component), and by magenta dashed lines (for absorption features of P Cygni profiles whenever possible). Note that, in contrast to Figs 4 and 5, the y-axes have different scales, to better see the shape of the broad components. Fluxes are in units of 10^{-16} erg s^{-1} cm^{-2} Å^{-1} and wavelengths are in Å.

2012, with small variations in the component fluxes. The width of the broad component remains unchanged until 2010 October with an FWHM ∼1000–1200 km s^{-1} (Table 2). After 2011, the flux and the velocity of the broad component markedly decreased. Furthermore, the absorption feature in the P Cygni profile disappeared towards the beginning of 2012. That disappearance together with the sharp decrease of the fluxes of the broad features are possibly due to the dense stellar envelope being destroyed and scattered.

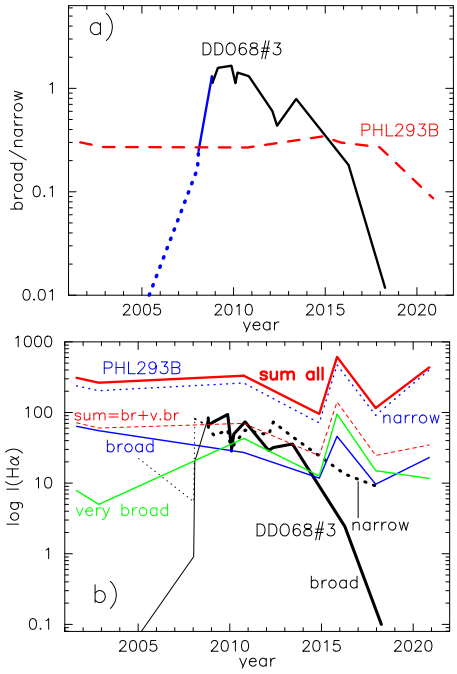

Figure 7. (a) Temporal variations of the flux ratio of broad-to-narrow H α components in DDO 68 #3. The black solid line shows the APO observations discussed here while the blue parts of the curve indicate Special Astrophysical Observatory and APO observations by Pustilnik, Kniazev & Pramskij (2005), Pustilnik et al. (2008) (dotted lines), and by Izotov & Thuan (2009) (solid line). The temporal variations of the same flux ratio in PHL 293B is shown by the red dashed line. Note that the total flux of the whole broad bump (i.e. the sum of the broad and very broad emission components, and of the absorption component when appropriate) was taken to be the broad component when calculating this broad-to-narrow ratio. (b) Temporal variations of H α fluxes in different components for DDO 68 #3. The thick black line shows the APO observations discussed here while the thin black line represents data by Pustilnik et al. (2005, 2008), and Izotov & Thuan (2009). The coloured lines show the data for PHL 293B.

In addition to the presence of broad components with absorption components, observed during the period from 2008 up to 2012 (Figs 4a–g), a low-intensity high-velocity redward tail made its appearance in 2012. It can be seen as a flux excess above the Gaussian fit to the broad component (Figs 4h and i). It should be noted, however, that the best fit to the 2012 profiles could only be obtained by including two Gaussians for the broad component (Fig. 5, a broad one and a very broad one). Thus, a supplementary broad component with a small FWHM = 300–500 km s^{-1} is present, in addition to the very broad component with a larger FWHM $\sim$ 1000 km s^{-1} (see Fig. 5, solid turquoise curves). Note the blueward shift in the broad components in Fig. 5 (solid turquoise curves). Likely, the appearance of the high-velocity tail and the subsequent disappearance of the P Cygni profile can be interpreted as the break-up of a dense circumstellar envelope by a rapid outflow. In 2013, the spectrum, despite being somewhat noisy, still clearly shows the broad blueward component (Fig. 4j). By 2018, the broad components have completely gone from the spectra, suggesting that the LBV shell has disappeared. The outburst event has thus lasted from 2008 to 2013, for a duration of about 5 yr.

Assuming that the broad components of the emission lines belong exclusively to the LBV, and that the narrow emission components are predominantly nebular, we can trace the decay of the LBV outburst by using the flux ratio of the broad-to-narrow components in each of the hydrogen and helium lines. This can be done most reliably for the brightest H α line. The temporal evolution of the H α broad-to-narrow flux ratio is shown in Fig. 7(a). A maximum for this flux ratio is seen between 2009 and 2010. It is more pronounced than the maximum for the flux of the broad component (Fig. 7b). However, in general, the variation of the broad-to-narrow flux ratio follows tightly the flux temporal evolution of the broad component.

To derive line flux luminosities for DDO 68, we need to know the distance of the dwarf galaxy. Based on the same imaging *HST* observations of the dwarf galaxy (GO 11578, PI: Aloisi), Cannon et al. (2014), Sacchi et al. (2016), and Makarov et al. (2017) have applied the TRGB (Tip of the Red Giant Branch) method to derive distances $D = 12.74$, 12.65, and 12.75 Mpc for DDO 68, respectively. New *HST* observations of a stream-like system associated with DDO 68 by Annibali et al. (2019b) give $D = 12.8 \pm 0.7$ Mpc, using the same TRGB method. The mean of these values is $D = 12.7$ Mpc, which we adopt. This distance is more than twice as large than the previous indirect distance determination of D $\sim$5–7 Mpc (NED) (see e.g. Pustilnik et al. 2005; Izotov & Thuan 2009).

With this distance, the luminosity of the H α broad component at the maximum is $\sim 2 \times 10^{38}$ erg s^{-1}. This maximum luminosity and the FWHM ($\sim$1000–1200 km s^{-1}) of the broad component of the lines during the transient event are in the ranges of those observed for LBV stars. The data thus suggest that an LBV star in the H II region DDO 68 #3 has undergone an outburst during the period 2008–2013.

The terminal velocity $v_{\rm term}$ of the LBV stellar wind is an important parameter for confronting theory with observation. It is obtained from the wavelength difference between the maximum of the broad emission line profile and the minimum of the blue absorption line profile. The terminal velocity $v_{\rm term}$ in DDO 68 #3 is of $\sim$800 km s^{-1} and does not change significantly over time (Table 2). It remains also unchanged during the 'maximum' of the eruption, as well as during the decay period starting in 2013. Nearly the same value of the expanding wind terminal velocity was reported by Izotov & Thuan (2009) and Pustilnik et al. (2017).

To summarize, the new data suggest that the broad component fluxes of the hydrogen lines of the LBV reached a maximum during the time interval $\sim$2008–2012. The narrow component also reached a maximum during the same period, but less pronounced. The broad-to-narrow component flux ratio reached a maximum at about the same period. This also supports the hypothesis that the LBV star underwent an eruptive event. It can be seen in Fig. 7 that the H α luminosity of the LBV star is now at a minimum or close to it.

3.3 PHL 293B

The situation with understanding the physical processes taking place in PHL 293B is more complex than in DDO 68 #3. PHL 293B (J2230–0006) is a well known SFG with a moderately low metallicity 12+logO/H $\sim$ 7.6–7.7 (e.g. Papaderos et al. 2008; Izotov et al. 2011; Fernández et al. 2018). Izotov & Thuan (2009) first detected a broad component in the strong hydrogen emission lines with P Cygni profiles of PHL 293B in a VLT UVES spectrum obtained on 2002 November 8, and in an SDSS spectrum taken on 2001 August 22. Those authors suggested that these broad features are due to a transient LBV phenomenon. Earlier observations of PHL 293B by Kinman (1965) and French (1980) did not mention any broad emission. The broad component was again detected by Izotov et al. (2011) in a VLT X-Shooter observation on 2009 August 16. Later observations have been carried out, and various other hypotheses have been proposed to interpret them. Thus, Terlevich et al. (2014) have suggested that the observations of PHL 293B can be explained

by a young dense expanding supershell driven by a stellar cluster wind and/or two supernova remnants or by a stationary wind. Hydrodynamic models have been built by Tenorio-Tagle et al. (2015).

On the basis of 10.4m GTC (Gran Telescopio Canarias)/MEGARA observations performed in 2017 July, Kehrig, Iglesias-Páramo & Vílchez (2020) found a flux ratio $I_{\rm br}/I_{\rm nar}$ ∼0.10 in the H α emission line of all integrated regions. They interpret this low value as due to a diminution of the broad H α emission.

Allan et al. (2020), from spectroscopic observations including the 2019 VLT X-Shooter data and radiation transfer modelling, report the absence of the broad emission component since 2011 and conclude that the LBV was in an eruptive state during 2001–2011 that has ended. Burke et al. (2021) also report the decrease of the $I_{\rm br}/I_{\rm nar}$ ratio from 0.41 (SDSS, 2001) to ∼0.10, using Gemini observations taken in 2019 December. Despite the fact that an AGN-like damped random walk model works well to fit the observed light curve, those authors concluded that a long-lived stellar transient of type SN IIn can better explain all the data for PHL 293B.

On the other hand, Prestwich et al. (2013) have emphasized the lack of X-ray emission in the galaxy, establishing an upper limit of $L_X \sim 3 \times 10^{38}$ erg s^{-1} (their table 6). This casts some doubt on the supernova model, thought to be the most probable one for explaining the PHL 293 phenomenon. Kehrig et al. (2020) have detected P Cygni profiles in the H α and H β emission lines in 2017 July, while those features were not found by Burke et al. (2020) in H α in 2019 December. These variations suggest that long-time monitoring, such as the observations described here, is important for distinguishing between various models.

Contrary to the conclusions of Izotov & Thuan (2009), based on the archival VLT/UVES observations on 2002-11-08, that P Cygni profiles are seen only in the hydrogen lines, and those of Terlevich et al. (2014), our new PHL 293B observations, as well as a reconsideration of the SDSS archival data (2001-08-22) and the VLT/X-Shooter observation by Izotov et al. (2011) on 2009-08-16, show that blue-shifted absorption lines are detected not only in hydrogen emission lines, but also in He I lines (Fig. 2). In other words, the situation is the same as in the case of DDO 68 #3 that has a much lower metallicity. However, the permitted Fe II emission lines, which generally originate in dense circumstellar envelopes and are usually seen in the spectra of LBV stars experiencing a giant eruption and creating an envelope, have not been detected in our new observations. Note that Terlevich et al. (2014) found blue-shifted Fe II absorption with a terminal velocity of ∼800 km s^{-1}. We did not detect permitted Fe II lines in the LBT spectrum obtained in 2020. Only forbidden [Fe III]λ λ4658, 4702, 4755:, 4986, 5270Å emission lines were found in this spectrum, with no absorption features.

In the decomposition of the strong emission lines, we have always attempted to fit the broad component in the simplest way possible, i.e. with the smallest number (preferably one) of Gaussian profiles. We also tried to perform fitting with Lorentzian profiles. But the results were always worse than in the case of Gaussian profiles. In the case of PHL293B, not one but two broad components are required to match the observed profiles well. The decomposition of H α for all spectra from Table 3 into narrow, broad, very broad (and absorption lines, whenever warranted), are presented in Fig. 6.

The P Cygni profile has persisted over some two decades, during the period 2001–2020, as is clearly seen in Fig. 2. The blueward absorption feature with wavelength ∼6545 Å is close to the nitrogen emission line [N II]λ6548 Å so that in many cases decomposition of the absorption profile in H α emission line is difficult. The absorption is likely present, but masked by strong broad and very broad components and the nitrogen emission line (Figs 3 and 6).

We obtain a high terminal velocity $v_{\rm term}$ ∼800 km s^{-1} for the absorption component in the Balmer lines. This value is the same as the ones derived by Izotov & Thuan (2009), Izotov et al. (2011), and Terlevich et al. (2014) from X-Shooter observations made in 2009 August and in 2009 August–September, respectively. The luminosity of the broad bump (i.e. the sum of broad and very broad components) varies from a few 10^{38} erg s^{-1} up to ∼10^{39} erg s^{-1}.

The very broad component derived by us from the SDSS spectrum taken in 2001 August (Fig. 6, Table 3) has nearly the same redshift as Terlevich et al. (2014)'s faint ultra-broad component measured from their 2009 observations and shown in their fig. 2 but a flux that is ∼100 times lower. Note that Terlevich et al. (2014) also fitted H α in their X-Shooter observation by two broad components. At about the same redshift, Izotov et al. (2011) also saw an excess in their fit of the H β broad component (their fig. 3). In our subsequent series of observations of PHL 293B starting in 2010, the very broad component does not show any redward shift. On the contrary, the broad and very broad components are centred practically at the systemic velocity of the galaxy. This means that, at least since 2010, there have been no large velocity outflows. We remark also that the broad components in the SDSS spectrum dated 2001 (Izotov & Thuan 2009), and in the VLT X-Shooter spectra dated 2009 (Izotov et al. 2011; Terlevich et al. 2014), have quite large FWHMs, ∼1500, 1000, and 1000 km s^{-1}, respectively. After 2010, these components become much narrower, with FWHM ∼ 160–180 km s^{-1}. This signifies the fact that the velocity dispersions of the moving and radiating matter have decreased, at least in the broad components.

If the ionization parameter is close to the limiting value of log$U \lesssim$–2, the radiation pressure can prevail over the ionized gas pressure (Dopita et al. 2002), and some contribution of a radiation-driven (i.e. by LyC and/or Ly α) superwind from a young stellar cluster, producing a high-velocity very broad component, will be possible (Komarova et al. 2021). To check this possibility, we use accurate oxygen abundance and an observational indicator of the ionization parameter, O32 = [O III] 4959,5007/[O II]3727, for PHL 293B (12 + logO/H = 7.72 and O32 = 15.52 from Izotov & Thuan 2009 and 12 + logO/H = 7.71 and O32 = 14.21 from Izotov et al. 2011) to estimate log$U$. We get (following Kobulnicky & Kewley 2004) log$U$ = –2.2 and log$U$ = –2.3, respectively, which are close to the maximum value, but still below it. Note that it is higher than log$U$ = –2.9 derived from the MMT observation by Izotov & Thuan (2009) for DDO 68 #3.

In general, the temporal variations of both the broad-to-narrow component flux ratios and of the H α fluxes of the narrow and broad components for PHL 293B (Fig. 7, coloured lines) are very different from those of DDO 68 #3 (Fig. 7, black lines). A strong variability of the H α fluxes, simultaneously in both the narrow and broad and very broad components, from 2011 to 2018, is seen in PHL 293B (Fig. 7b). Flux jumps by a factor of ∼6 are observed in both the narrow and the sum of the broad and very broad components (Table 3). We have checked the logs of the observations and have determined that all observations were carried out in photometric conditions, so that the flux variations cannot be attributed to sky variability. The flux variations, both in the narrow and broad and even very broad components (a sharp flux decrease in 2014 followed by a rise at the end of 2015, followed by another decrease in 2017) can be explained by inaccurate pointing when observing with a narrow slit of 0.9 arcsec. However, the variations are likely to be real because the light curves derived by Burke et al. (2021) from SDSS and DES (Dark Energy Survey) imaging between 1998 and 2018 (their fig. 2) also show small-amplitude variability in the g and r bands during the same years. The synchronicity in the variability of fluxes in the

narrow and broad components does not hold anymore starting 2018 (see also the fading of the broad component in Allan et al. 2020; Burke et al. 2021).

In contrast to the outburst nature of the variability over time of the broad-to-narrow flux ratio in DDO 68 #3, which manifests itself in the form of a peak (Fig. 7a, black line), PHL 293B does not undergo such type of variation. Its broad-to-narrow flux ratios depend weakly on time, at least over the past two decades. However, a decrease in the broad-to-narrow flux ratio can be seen starting from the very end of 2017 and continuing to 2020 (Fig. 7a). This decrease can be partly explained by an increase of the narrow component relative to the broad one (Fig. 7b, blue and red dashed and green solid lines).

In the case of PHL 293B, the behaviour of the broad component may be explained by several effects. Enduring broad hydrogen Balmer P Cygni profiles with absorption feature blue-shifted by $\sim$800 km s^{-1}, can indicate the presence of fast moving ejecta. The persistent luminosity of the broad Balmer emission and the possibility that the Balmer emission could be due to a long-lived stellar transient, like LBV/SN, motivate additional follow-up spectroscopy to distinguish between these effects.

3.4 LBVs in other SFGs

We now compare the behaviour of the candidate LBVs in DDO 68 #3 and PHL 293B with those in other SFGs.

The LBV in the relatively low-metallicity galaxy Mrk 177 = UGCA 239 at the post-merger stage, with 12 + logO/H = 8.58 and D_L = 28.9 Mpc, has undergone multiple outbursts during the last 20 yr (Kokubo 2021). The luminosity of the broad H α component of Mrk 177 varies from a maximum of 10^{40} erg s^{-1} during the strongest explosion to 10^{39} erg s^{-1} during the next two strong explosions. This is an order of magnitude higher than the corresponding values of L(H α) (broad) = (2–9) $\times$ 10^{38} erg s^{-1} in PHL 293B. As for the H α broad-to-narrow flux ratio for the LBV in Mrk 177, it varies in the interval 3.4–4.5 during last two outbursts. This is in the same range as the LBV outburst maximum in DDO 68 #3, but one order of magnitude higher than in PHL 293B. The strongest outburst in Mrk 177 during 2001 is characterized by a H α broad-to-narrow ratio that is approximately 10 times higher than those during subsequent explosions, i.e. $\sim$two orders of magnitude higher than in PHL 293B.

On the other hand, the luminosity L(H α) $\sim$$10^{38}$ erg s^{-1} (Drissen et al. 2001) of the LBV-V1 in the low-metallicity (12 + logO/H = 7.89; Izotov, Thuan & Lipovetsky 1997) galaxy Mrk 71 (NGC 2363A) is lower than that of the cLBV in PHL 293B, with a similar metallicity.

4 CONCLUSIONS

Over nearly two decades, we have monitored the time variation of the broad component fluxes and of the broad-to-narrow flux ratios of the strong hydrogen and helium emission lines in two low metallicity SFGs, DDO 68 (12 + logO/H = 7.15) and PHL 293B (12 + logO/H = 7.72). These two SFGs have the particularity of harbouring cLBV stars. We have carried out this monitoring by obtaining over time spectra of these two objects with the 3.5m APO telescope and the 2 $\times$ 8.4m LBT. Our main results are the following:

(1) The broad emission with a P Cygni profile of the H α line emitted by the DDO 68 H II region #3 shows a marked increase of its luminosity during the period 2005 to 2017, reaching a maximum L(H α) of $\sim$$10^{38}$ erg s^{-1} in 2008–2011, adopting the distance derived from brightness of the TRGB. The absorption feature of the P Cygni-like profile and the broad component rapidly decayed and disappeared in 2018. These properties are characteristic of an eruptive event in an LBV star. The derived H α luminosity and the FWHM $\sim$1000–1200 km s^{-1} of the broad component during the eruption event are in the range of those observed for LBV stars. A terminal velocity $v_{\rm term}$ $\sim$800 km s^{-1} is measured from the absorption profile. It does not change significantly over time. These observations are also consistent with the earlier findings of Pustilnik et al. (2017) who described the LBV in DDO 68 #3 as going through a fading phase during 2015–2016, and with those of Annibali et al. (2019a) who did not find any characteristic sign of an LBV star at the beginning of 2017. Thus, our spectroscopic monitoring indicates that the LBV has passed through the maximum of its eruption activity and is now in a fairly quiet phase.

(2) The situation is quite different in the BCD PHL 293B. Since the discovery of the cLBV in it on the basis of SDSS 2001 observations, the fluxes of the broad component and the broad-to-narrow flux ratios of the hydrogen emission lines in PHL 293B have remained nearly constant, with small variations, over 16 yr, at least until 2015. A decrease of the broad-to-narrow flux ratio in recent years (2017–2020) can partly be attributed to an increase of the narrow component flux relative to that of the broad component. The luminosity of the broad H α component varies from $\sim$2 $\times$ 10^{38} erg s^{-1} to $\sim$$10^{39}$ erg s^{-1}, and the FWHM varies in the range $\sim$500–1500 km s^{-1} over the whole period of monitoring of PHL 293B, from 2001 to 2020.

Unusually persistent P Cygni features with broad and very broad components of hydrogen emission lines and blueward absorption in the H I and He I emission lines are clearly visible, even at the very end of 2020, despite the several decreases of the broad-to-narrow flux ratio in the most recent years (2017–2020). A terminal velocity $v_{\rm term}$ $\sim$800 km s^{-1} is measured in PHL 293B, similar to the one obtained for DDO 68 #3, although the latter is 3.7 times more metal deficient than the former. The terminal velocity does not change significantly with time. The near-constancy of the H α flux suggests that the cLBV in PHL 293B is a long-lived stellar transient of type LBV/SN IIn. However, other mechanisms such as a stationary wind from a young stellar cluster, cannot be ruled out. Further spectroscopic time monitoring of the BCD is needed to narrow down the nature of the phenomenon in PHL 293B.

ACKNOWLEDGEMENTS

NGG and YII acknowledge support from the National Academy of Sciences of Ukraine (Project No. 0121U109612 'Dynamics of particles and collective excitations in high energy physics, astrophysics and quantum microsystem'). TXT thanks the hospitality of the Institut d'Astrophysique in Paris where part of this work was carried out. The Apache Point Observatory (APO) 3.5m telescope is owned and operated by the Astrophysical Research Consortium (ARC). The Large Binocular Telescope (LBT) is an international collaboration among institutions in the United States, Italy, and Germany. LBT Corporation partners are: The University of Arizona on behalf of the Arizona university system; Istituto Nazionale di Astrofisica, Italy; LBT Beteiligungsgesellschaft, Germany, representing the Max-Planck Society, the Astrophysical Institute Potsdam, and Heidelberg University; The Ohio State University, and The Research Corporation, on behalf of The University of Notre Dame, University of Minnesota and University of Virginia. This paper used data obtained with the Multi-Object Double Spectrographs (MODS) spectrographs built with funding from National Science Foiundation (NSF) grant AST-9987045 and the NSF Telescope System Instrumentation Program (TSIP), with additional funds from the Ohio Board of Regents and the Ohio State University Office

of Research. IRAF is distributed by the National Optical Astronomy Observatories, which are operated by the Association of Universities for Research in Astronomy, Inc., under cooperative agreement with the National Science Foundation. Funding for the Sloan Digital Sky Survey (SDSS) IV has been provided by the Alfred P. Sloan Foundation, the U.S. Department of Energy Office of Science, and the Participating Institutions. SDSS-IV acknowledges support and resources from the Center for High-Performance Computing at the University of Utah. The SDSS website is www.sdss.org. SDSS-IV is managed by the Astrophysical Research Consortium for the Participating Institutions of the SDSS Collaboration. This research has made use of the NASA/IPAC Extragalactic Database (NED), which is operated by the Jet Propulsion Laboratory, California Institute of Technology, under contract with the National Aeronautics and Space Administration.

DATA AVAILABILITY

The data underlying this article will be shared on reasonable request to the corresponding author.

REFERENCES

Allan A. P., Groh J. H., Mehner A., Smith N., Boian I., Farrell E. J., Andrews J., 2020, MNRAS, 496, 1902
Annibali F. et al., 2019a, MNRAS, 482, 3892
Annibali F. et al., 2019b, ApJ, 883, 19
Burke C. J. et al., 2020, ApJ, 894, L5
Burke C. J., Liu X., Chen Y.-C., Shen Y., Guo H., 2021, MNRAS, 504, 543
Cannon J. M. et al., 2014, ApJ, 787, L1
Crowther P. A., 2007, ARA&A, 45, 177
Davidson K., 1999, in Morse J. A., Humphreys R. M., Damineli A., eds, ASP Conf. Ser. Vol. 179, 'Eta Carinae At The Millennium'. Astron. Soc. Pac., San Francisco, p. 6
Davidson K., Humphreys R. M., 1997, ARA&A, 35, 1
Dopita M. A., Groves B. A., Sutherland R. S., Binette L., Cecil G., 2002, ApJ, 572, 753
Drissen L., Roy J.-R., Robert C., 1997, ApJ, 474, L35
Drissen L., Crowther P. A., Smith L. J., Robert C., Roy J.-R., Hillier D. J., 2001, ApJ, 546, 484
Fernández V., Terlevich E., Díaz A., Terlevich R., Rosales-Ortega F. F., 2018, MNRAS, 478, 5301
French H. B., 1980, ApJ, 240, 41
Grassitelli L, Langer N., Mackey J., Gräfener G., Grin N. J., Sander A. A. C., Vink J. S., 2020, A&A, 647, 99
Guseva N. G., Izotov Y. I., Thuan T. X., 2000, ApJ, 531, 776
Guseva N. G., Izotov Y. I., Fricke K. J., Henkel C., 2012, A&A, 541, A115
Humphreys R. M., 2019, Galaxies, 7, 75
Humphreys R. M., Davidson K., 1994, PASP, 106, 1025
Humphreys R. M., Davidson K., Grammer S., Kneeland N., Martin J. C., Weis K., Burggraf B., 2013, ApJ, 773, 46
Humphreys R. M., Davidson K., Hahn D., Martin J. C., Weis K., 2017, ApJ, 844, 40
Izotov Y. I., Thuan T. X., 2008, ApJ, 687, 133
Izotov Y. I., Thuan T. X., 2009, ApJ, 690, 1797
Izotov Y. I., Thuan T. X., Lipovetsky V A., 1994, ApJ, 435, 647
Izotov Y. I., Thuan T. X., Lipovetsky V. A., 1997, ApJS, 108, 1
Izotov Y. I., Thuan T. X., Guseva N. G., 2007, ApJ, 671, 1297
Izotov Y. I., Guseva N. G., Fricke K. J., Henkel C., 2011, A&A, 533, A25
Kehrig C. et al., 2020, MNRAS, 498, 1638
Kinman T. D., 1965, ApJ, 142, 1241
Kobulnicky H. A., Kewley L. J., 2004, ApJ, 617, 240
Kokubo M., 2021, MNRAS, preprint (arXiv:2101.07797)
Komarova L., Oey M. S., Krumholz M. R., Silich S., Kumari N., James B. L., 2021, ApJ, 920, L46
Lamers H. J. G. L. M., de Groot M., Cassatella A., 1983, A&A, 128, 299
Leitherer C., Leão J. R. S., Heckman T. M., Lennon D. J., Pettini M., Robert C., 2001, ApJ, 550, 724
Makarov D. I., Makarova L. N., Pustilnik S. A., Borisov S. B., 2017, MNRAS, 466, 556
Massey P., Waterhouse E., DeGioia-Eastwood K., 2000, AJ, 119, 2214
Papaderos P., Guseva N. G., Izotov Y. I., Fricke K. J., 2008, A&A, 491, 113
Pogge R., 2019, https://doi.org/10.5281/zenodo.2550741
Prestwich A. H., Tsantaki M., Zezas A., Jackson F., Roberts T. P., Foltz R., Linden T., Kalogera V., 2013, ApJ, 769, 92
Pustilnik S. A., Kniazev A. Y., Pramskij A. G., 2005, A&A, 443, 91
Pustilnik S. A., Tepliakova A. L., Kniazev A. Y., Burenkov A. N., 2008, MNRAS, 388, L24
Pustilnik S. A., Makarova L. N., Perepelitsyna Y. A., Moiseev A. V., Makarov D. I., 2017, MNRAS, 465, 4985
Sacchi E. et al., 2016, ApJ, 830, 3
Schaerer D., Contini T., Pindao M., 1999, A&AS, 136, 35
Smith L. J., Crowther P. A., Prinja R. K., 1994, A&A, 281, 833
Smith N., Li W., Silverman J. M., Ganeshalingam M., Filippenko A. V., 2011, MNRAS, 415, 773
Sobral D. et al., 2018, MNRAS, 477, 2817
Solovyeva Y. et al., 2020, MNRAS, 497, 4834
Tenorio-Tagle G., Silich S., Martínez-González S., Terlevich R., Terlevich E., 2015, ApJ, 800, 131
Terlevich R., Terlevich E., Bosch G., Díaz Á., Hägele G., Cardaci M., Firpo V., 2014, MNRAS, 445, 1449
Vink J. S., 2012, in Humphreys R., Davidson K., eds, Astrophysics and Space Science Library, Vol. 384, 'Eta Carinae and the Supernova Imposters'. Springer-Verlag, Berlin, p. 221
Weis K., Bomans D. J., 2020, Galaxies, 8, 20
Wofford A. et al., 2020, MNRAS, 493, 2410

This paper has been typeset from a TEX/LATEX file prepared by the author.